



SACLANT ASW
RESEARCH CENTRE
REPORT

SOUND PROPAGATION IN SHALLOW WATER:
A DETAILED DESCRIPTION OF THE ACOUSTIC FIELD
CLOSE TO SURFACE AND BOTTOM

by

FINN B. JENSEN

1 FEBRUARY 1981

NORTH
ATLANTIC
TREATY
ORGANIZATION

LA SPEZIA, ITALY

This document is unclassified. The information it contains is published subject to the conditions of the legend printed on the inside cover. Short quotations from it may be made in other publications if credit is given to the author(s). Except for working copies for research purposes or for use in official NATO publications, reproduction requires the authorization of the Director of SACLANTCEN.

This document is released to a NATO Government at the direction of the SACLANTCEN subject to the following conditions:

1. The recipient NATO Government agrees to use its best endeavours to ensure that the information herein disclosed, whether or not it bears a security classification, is not dealt with in any manner (a) contrary to the intent of the provisions of the Charter of the Centre, or (b) prejudicial to the rights of the owner thereof to obtain patent, copyright, or other like statutory protection therefor.

2. If the technical information was originally released to the Centre by a NATO Government subject to restrictions clearly marked on this document the recipient NATO Government agrees to use its best endeavours to abide by the terms of the restrictions so imposed by the releasing Government.

SACLANTCEN REPORT SR-57

NORTH ATLANTIC TREATY ORGANIZATION
SACLANT ASW Research Centre
Viale San Bartolomeo 400, I-19026 San Bartolomeo (SP), Italy.

tel: national 0187 560940
international + 39 187 560940

telex: 271148 SACENT I

SOUND PROPAGATION IN SHALLOW WATER:
A DETAILED DESCRIPTION OF THE ACOUSTIC FIELD CLOSE TO SURFACE AND BOTTOM

by

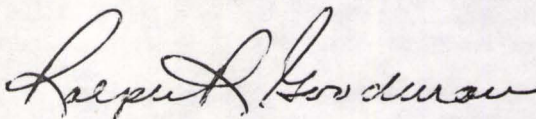
Finn B. Jensen

(Reprinted from J. Acoustical Society America 70, 1981: 1397-1406)

1 February 1982

This report has been prepared as part of Project 19.

APPROVED FOR DISTRIBUTION



RALPH R. GOODMAN
Director

Sound propagation in shallow water: A detailed description of the acoustic field close to surface and bottom

Finn B. Jensen

SACLANT ASW Research Centre, 19026 La Spezia, Italy
(Received 9 April 1981; accepted for publication 27 July 1981)

Experimental data are compared with normal-mode predictions for an isovelocity shallow-water propagation channel overlying a complicated layered bottom. Measurements were made close to both the sea surface and the sea floor with a vertical hydrophone spacing of 1 m. Excellent agreement between theory and experiment is obtained over the frequency range 50–3200 Hz and for ranges up to 30 km. Some problems associated with deterministic modeling are also discussed and appropriate solutions are indicated.

PACS numbers: 43.30.Bp, 43.30.Jx, 91.50.Ey, 92.10.Vz

INTRODUCTION

A series of studies¹⁻¹⁰ on the applicability of normal-mode theory to sound propagation in shallow water has appeared in the last decade. The earlier papers¹⁻⁵ were mainly concerned with the verification of single-mode properties by comparison with experimental data at a few frequencies. Then some papers^{6,7} appeared where mode theory was compared with broadband experimental data for range-independent environments, and recently⁸⁻¹⁰ adiabatic mode theory has been successfully applied to broadband propagation in range-dependent shallow-water environments.

When dealing with shallow-water data for the purpose of verifying a particular propagation model, it is important to use data from the near-surface and near-bottom fields, since the acoustic field there is much more sensitive to environmental parameters than is the field at mid-depth. In a previous paper⁶ we compared normal-mode theory with a broadband data set comprising a near-surface (2 m) and a mid-depth (50 m) receiver. The present study is an extension hereof with a much better sampling of the acoustic field over depth. Thus, in addition to a sample point at mid-depth, the field has been sampled every 1 m within the first 10 m of both the sea surface and the sea floor.

The model/data comparison presented in this paper has the specific purpose of verifying a propagation model¹¹ based on normal-mode theory. In addition, some general problems associated with deterministic modeling are addressed and appropriate solutions are indicated. Section I describes the experimental setup and the environmental conditions during the experiment. The acoustic model is described in Sec. II, and Sec. III deals with the actual model/data comparison. The conclusions of this study are given in Sec. IV. Finally, the Appendix is dedicated to problems associated with deterministic modeling, such as coherent versus incoherent addition of modes, band averaging, and a phenomenon called channel resonance.

I. EXPERIMENTAL PROCEDURES

The experimental data¹² were collected in March 1975 in a standard shallow-water area close to the island of Elba, off the Italian west coast, where environmental conditions are well-known from earlier experiments.¹³ The bathymetry and the trial track are shown in Fig. 1.

The track is approximately 30 km long over an almost constant water depth of about 115 m. A schematic of the experimental setup is given in Fig. 2. Two ships were employed. The receiving ship, shown to the right, was anchored at a fixed position, while a smaller ship, sailing away from the receiving ship, dropped explosive charges at regular intervals over ranges up to 30 km. The charges (180 g of TNT) were set to fire at 50-m depth.

Two runs were made. One with the receiving array placed close to the surface (attached to a surface buoy) and one with the array placed close to the bottom. The two array positions are shown in Fig. 2. The array consists of nine hydrophones placed 1 m apart, and the first hydrophone was in both cases placed 1 m away from the boundary. In both runs an extra hydrophone was suspended at mid-depth for checking reproducibility of the data. The recorded broadband signals were processed onboard the receiving ship, and transmission loss was calculated for $\frac{1}{3}$ -octave bands with center frequencies ranging from 50 Hz to 3.2 kHz.

The experiments were carried out in almost isothermal water under moderately rough sea conditions with winds averaging 15–20 knots during the two runs. A representative "average" bottom for the trial zone was determined in the following way. First, a rough

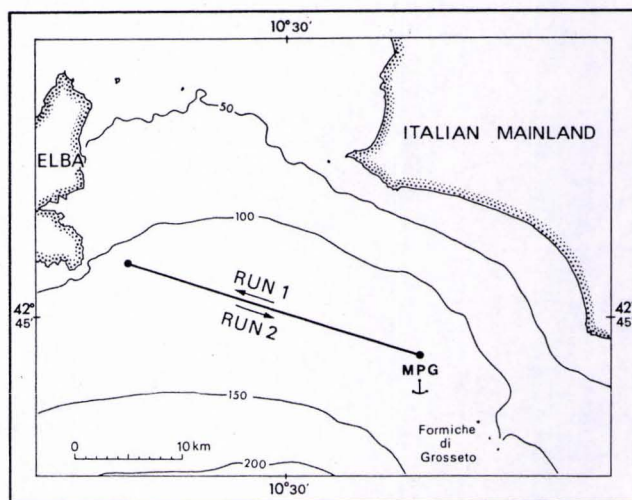


FIG. 1. Bathymetry and trial track.

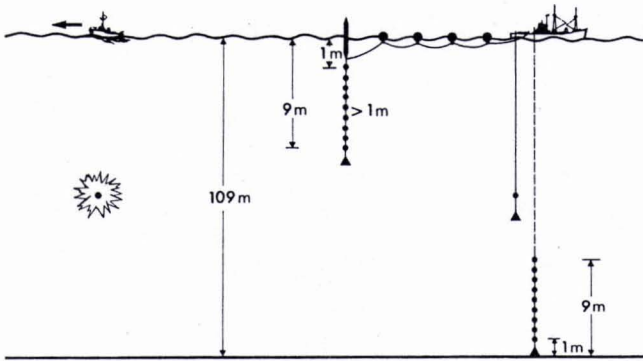


FIG. 2. Experimental setup.

estimate of the bottom structure was obtained from cores and seismic profiling experiments. Second, propagation data taken in the same area during the years 1969–70 were used in an extensive model/data comparison to obtain a detailed bottom description.¹³ This second step was necessary for a full physical description of the bottom, since properties such as wave attenuation and shear speed cannot easily be determined from cores and seismic experiments.

Figure 3 shows the sound-speed structure obtained from three cores from the trial zone, while Fig. 4 shows the “average” bottom determined on the basis of the model/data comparison.¹³ The bottom essentially consists of a 6-m thick sediment layer (clay) overlying a harder subbottom (sand). Note that the low-speed sediment layer has a high-speed sand layer embedded in it, a feature seen also in the core result shown in Fig. 3.

As pointed out above, bottom properties have been determined through a model/data comparison using earlier summer and winter data with source and receiver around mid-depth. In the present study we are using the same acoustic model and the same bottom structure, but here applied to a new data set that includes measurements close to both the sea surface and the sea floor. Hence, a good agreement between theory and experiment would indicate both that an appropriate “average” bottom has been found,¹³ and that the normal-mode model provides an adequate description of sound propagation in this particular area.

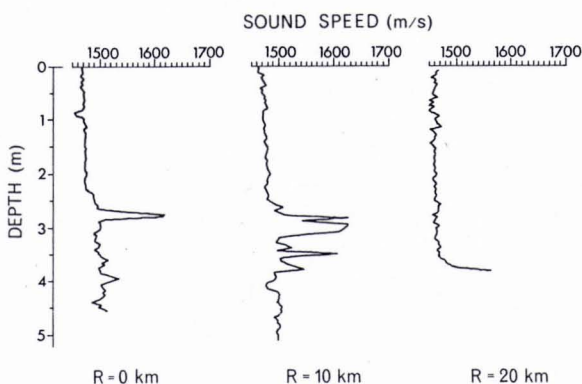


FIG. 3. Sound-speed structure in bottom measured from cores.

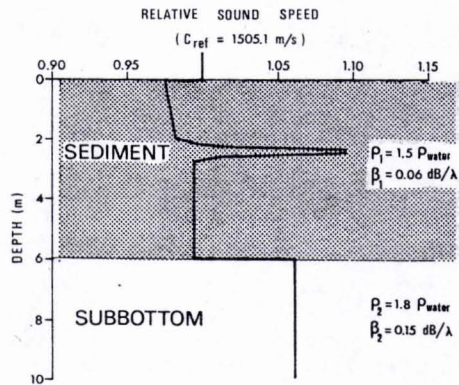


FIG. 4. Bottom parameters used as input to propagation model.

II. THE ACOUSTIC MODEL

Of the various acoustic models¹⁴ suited for handling propagation in shallow water, we have chosen to exercise a normal-mode model. This model¹¹ treats the ocean as two fluid layers (water and sediment) overlying a semi-infinite solid subbottom. The sound speed in both fluid layers is allowed to vary arbitrarily with depth, while density and compressional wave attenuation are taken to be constant within each layer. In the semi-infinite subbottom all properties are constant with depth, i.e., compressional speed and attenuation, shear speed and attenuation, and density. For a given source frequency the model computes the acoustic field (transmission loss) versus depth and range in a purely deterministic fashion by either coherent or incoherent addition of modes. Some problems associated with a purely deterministic calculation of the acoustic field are addressed in the Appendix.

The environment is taken to be range-independent, and the actual numerical values used as input to the model are the following: a water depth of 109 m, a density of 1 g/cm^3 , and a frequency-dependent volume attenuation.¹⁵ Bottom properties are given in Fig. 4, where β is the compressional wave attenuation in dB per wavelength. Because of the muddy nature of the bottom no shear wave effects were considered.

III. MODEL/DATA COMPARISON

Before proceeding to a detailed comparison of computed and measured acoustic fields, we will anticipate the general field behavior versus depth, range, and frequency by some simple physical considerations. First of all, we expect propagation loss to increase with range and frequency due to volume attenuation in the water. However, at sufficiently low frequencies the effect of channel cutoff also leads to high losses resulting in an intermediate frequency being the optimum frequency of propagation. In general the optimum frequency depends on both range and source/receiver depth. Secondly, we expect the acoustic field over depth to be asymmetric due to different boundary conditions at the surface and the bottom. The surface is taken to be pressure release, and consequently, the propagation loss close to the surface is expected to be very high. What is meant by “close to the surface”

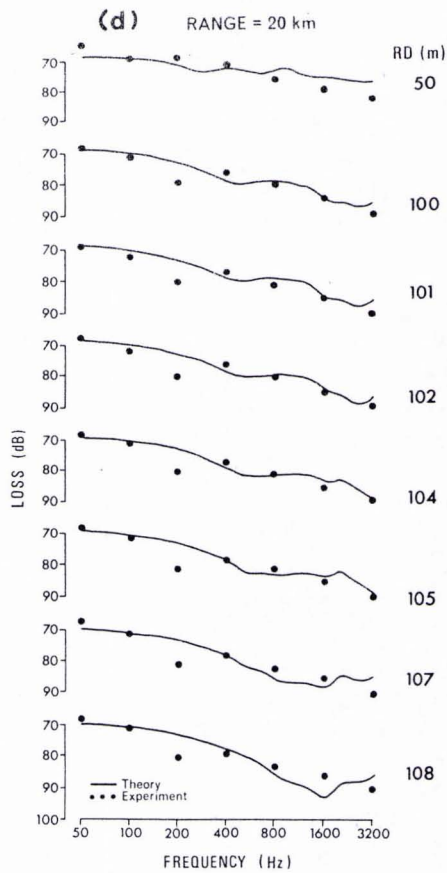
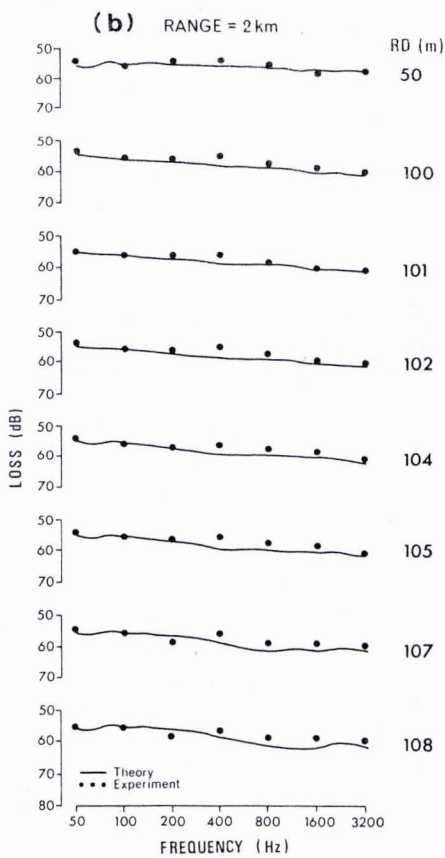
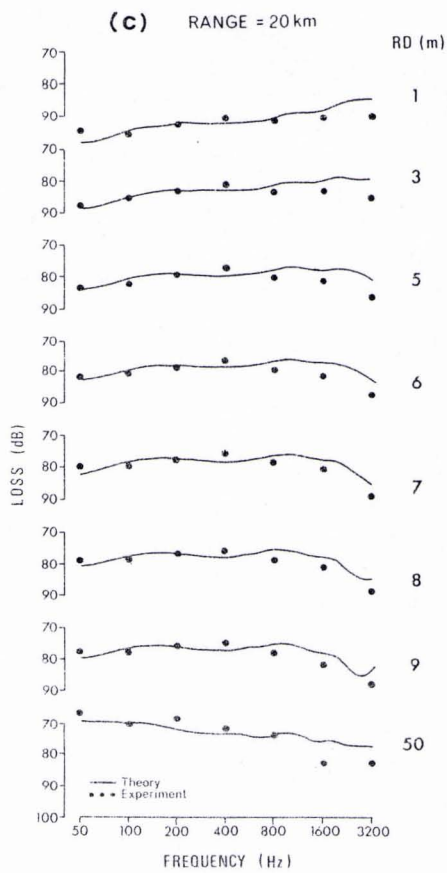
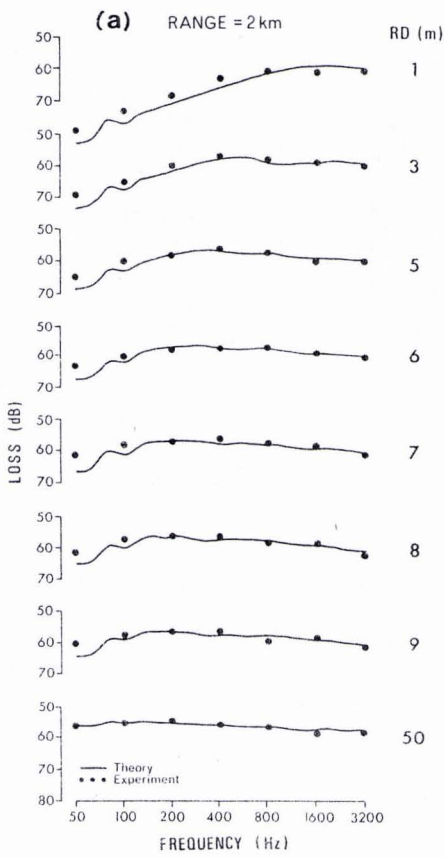


FIG. 5. Loss versus frequency close to surface and bottom at short and long ranges.

will depend on frequency, refraction conditions, range between source and receiver, and also on the bottom properties. The bottom is taken to be a fluid with properties not too different from those of water. Therefore no drastic change in the acoustic field is expected when approaching the bottom. Actually, we would expect the field in the lower part of the water column to be relatively constant with depth.

Finally, all data presented below are $\frac{1}{3}$ -octave averaged, and the frequencies given in the figures are center frequencies for the $\frac{1}{3}$ -octave bands. The theoretical curves have been obtained as described in the Appendix, i. e., we have simulated third-octave results and eliminated "channel resonance." The notation used is F (frequency), R (range), SD (source depth), and RD (receiver depth).

A. Field behavior versus frequency

The display chosen in Fig. 5(a) clearly shows the frequency-dependent behavior of the acoustic field. The model/data comparison is here done close to the source ($R=2$ km), and we consider the field close to the sea surface as compared to a mid-water receiver. Note the excellent agreement between theory (line) and experiment (dots) for all receiver depths. One meter below the surface the optimum frequency is seen to be around 1600 Hz with a 20-dB better propagation than at 50 Hz. Moving away from the surface all frequencies seem to propagate equally well, a fact also confirmed by Fig. 5(b), which displays the acoustic field close to the bottom. Thus, at short ranges where attenuation effects are relatively unimportant, the field behavior is dominated by the pressure-release boundary condition, which causes a frequency-dependent intensity falloff close to the sea surface.

The field behavior versus frequency at a range of 20 km is shown in Figs. 5(c) and (d). Here there is only little frequency dependence close to the sea surface [Fig. 5(c)], while the propagation loss clearly increases with frequency in the lower part of the water column [Fig. 5(d)]. Thus the propagation loss at 50 Hz is around 20 dB lower than at 3.2 kHz. This change in field behavior with range is caused by the bottom loss, which for a layered bottom is frequency dependent and therefore has a complicated influence on the acoustic field.

This series of figures clearly demonstrates the complicated behavior of the acoustic field versus depth, range, and frequency. However, we note that all features exhibited by the experimental data are accurately described by the normal-mode model.

B. Field behavior versus depth

Figure 6 shows the field intensity over depth at selected frequencies for two different ranges, 2 and 20 km. Note that the depth axis is interrupted. The graphs only show the first and the last 10 m of the water column plus a small interval around 50-m depth. The line is theory and the dots experimental data. We see that the loss in the lower part of the water column

is almost independent of depth at all frequencies, while the loss generally increases considerably when approaching the sea surface. Thus, at the lowest frequencies [Figs. 6(a) and (b)], the propagation loss 1 m below the surface is around 25 dB higher than at mid-depth. We also notice that the thickness of the "acoustic boundary layer," defined as the region below the surface with strong intensity falloff, decreases with increasing frequency. At 50 Hz [Fig. 6(a)] the intensity is low within the first 10–20 m of the surface as compared to the level at mid-depth. On the other hand, at 3.2 kHz and at short ranges [Fig. 6(g)] the insonification is almost constant on all receivers, meaning that the boundary layer here is less than 1 m thick. Thus the boundary layer thickness is to a first approximation of the order of an acoustic wavelength, with some dependence on range.

In terms of normal-mode theory, the insonification near the sea surface is determined by the total number of modes present at any given frequency. Thus, at lower frequencies, few modes exist and the boundary layer is thick. At higher frequencies many modes exist and the boundary layer is thin because the higher-order modes have higher derivatives at the surface, i. e., their amplitudes fall off rapidly but only near the surface. However, at longer ranges the higher-order modes tend to be stripped off due to bottom attenuation, which in turn results in a thickening of the boundary layer with range. This mode-stripping effect is particularly evident at intermediate and higher frequencies [Figs. 6(e)–(g)].

The above sequence of figures shows excellent agreement between theory and experiment. We see that the optimum propagation conditions are generally obtained with the receiver at the same depth as the source (50 m). Combining this information with the information on optimum frequency from the previous section, the best propagation in this particular environment is obtained for a frequency of 50 Hz with source and receiver both at 50 m.

C. Field behavior versus range

In Fig. 7 we show unsmoothed propagation data versus range at selected frequencies. Here the number of shots per trial can also be seen. The three figures are for the receiver 1 m below the surface, at mid-depth, and 1 m above the bottom, respectively. We see that the agreement between theory and experiment is good with a maximum deviation of about 5 dB when considering mean levels. This is an extremely good agreement for data covering the entire water column, a range of 30 km, and 6 octaves of frequency.

To demonstrate more explicitly the success with which propagation in this area has been modeled, we show in Fig. 8 loss versus range at 100 Hz for both a mid-depth receiver and a receiver 1 m below the surface. Note that both model and data show a level difference between the two hydrophones of 20–25 dB over the entire range of 30 km. This shows that the distribution of energy within the water column is accurately handled by the normal-mode model. Likewise, the fre-

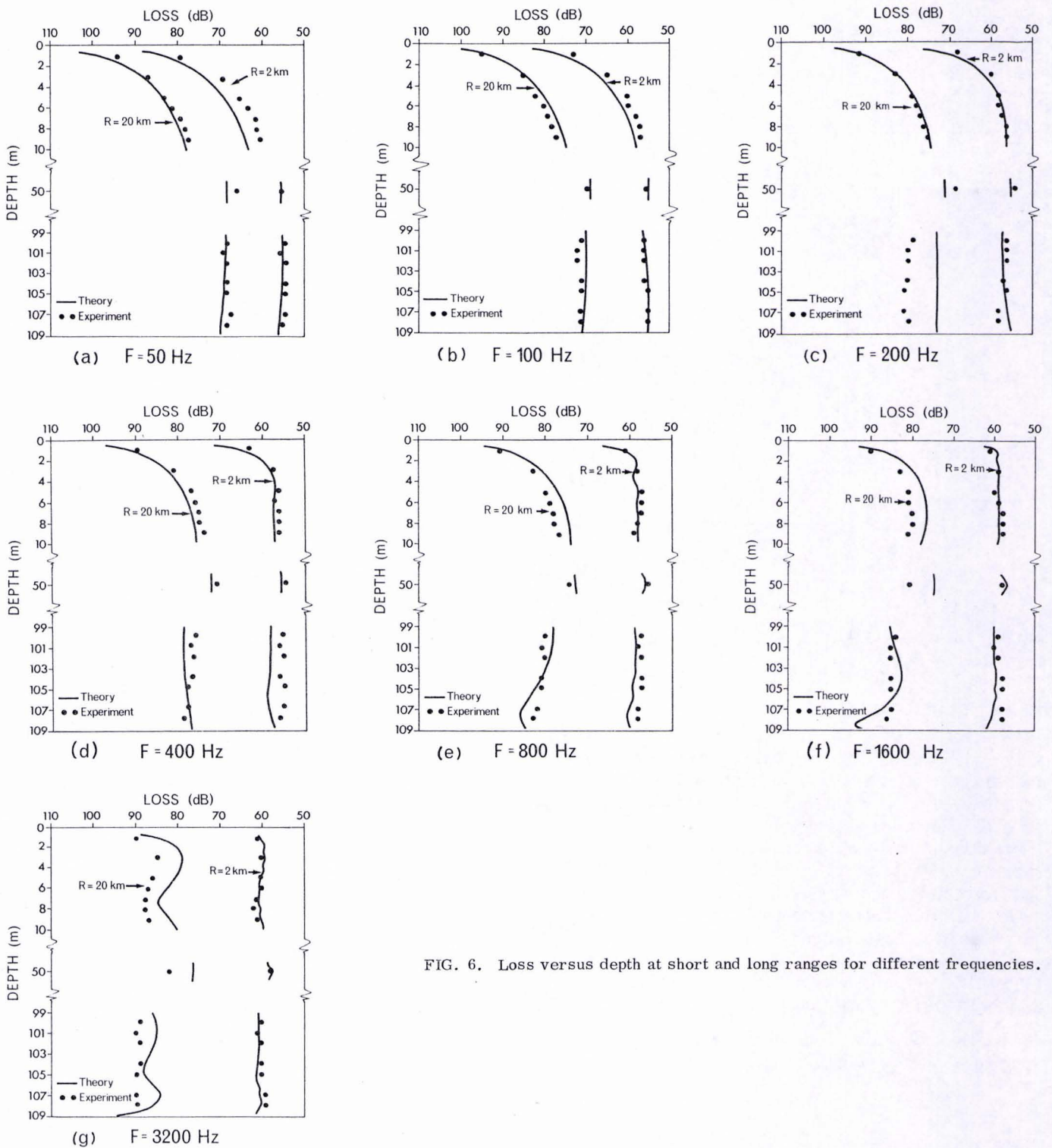


FIG. 6. Loss versus depth at short and long ranges for different frequencies.

quency dependence of shallow-water propagation is also accurately handled by the model, which is demonstrated in Fig. 9. Here loss is shown for a receiver 1 m above the bottom for two frequencies, 50 and 3200 Hz. The level difference is here approximately 25 dB at 30 km, with the lowest loss at 5 Hz. Note how the experimental data for 3.2-kHz drop below the theoretical curve beyond a range of 15 km. This sudden increase in propagation loss of around 5 dB is probably due to changing bottom characteristics beyond 15 km. The

phenomenon is consistent in the data for higher frequencies, but only for receivers close to the bottom. The good agreement found between theory and experiment in this study is somewhat unusual in shallow-water acoustic modeling. Generally, the difficulties encountered when trying to match model predictions with broadband experimental data are substantial,⁶⁻¹⁰ dependent, of course, on the complexity of the ocean environment and on the amount of initial environmental information available.

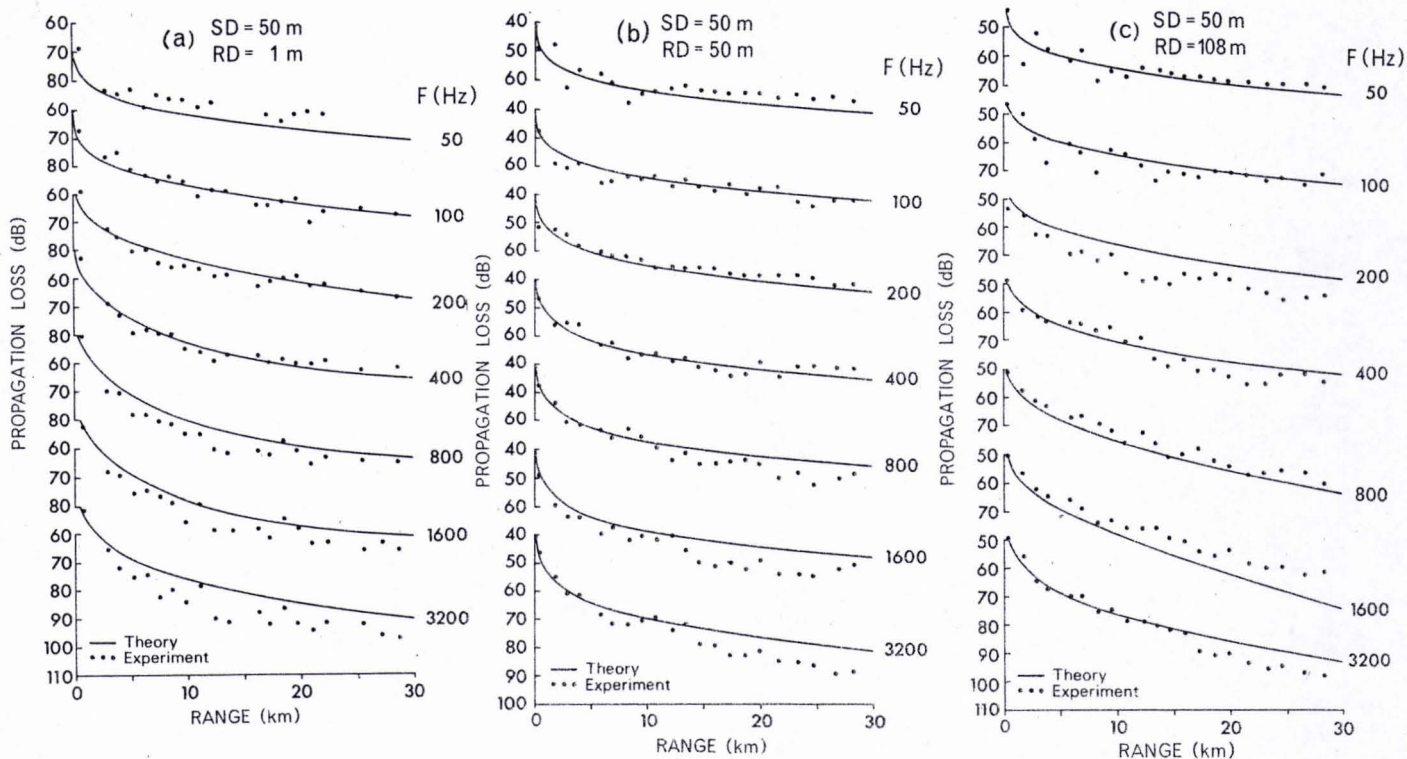


FIG. 7. Loss versus range 1 m below the surface, at mid-depth and 1 m above the bottom.

IV. CONCLUSIONS

Remarkably good agreement is found between theory and experiment for data covering the entire water column, a range of 30 km, and 6 octaves of frequency in a shallow-water area. The main features exhibited by the experimental data concerning optimum frequency of propagation at various ranges and depths are accurately predicted by the acoustic model. This in turn means that the confidence gained earlier in the use of normal-mode theory for modeling sound propagation in shallow water has been further strengthened.

APPENDIX: PROBLEMS ASSOCIATED WITH DETERMINISTIC MODELING

A purely deterministic model treats sound propagation problems in a simplified manner allowing only for

completely regular well-defined propagation paths through the ocean. Particularly a range-independent model has this defect since it treats the ocean as horizontally stratified. The normal-mode model used in this study is such a deterministic model giving simplified answers to propagation in the ocean. Some of the problems associated with deterministic modeling will be addressed here, particularly in the context of model/data comparisons, where the data are averaged over third-octave bands.

A. Coherent versus incoherent addition of modes

A normal-mode model generally allows for both coherent and incoherent addition of modes. However, only the coherent loss computation is a true deterministic representation of the acoustic field with full phase

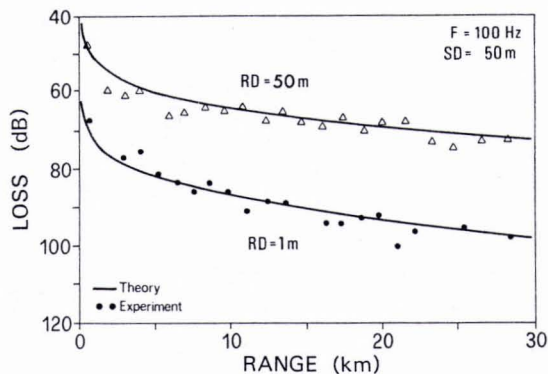


FIG. 8. Loss versus range at two different receiver depths.

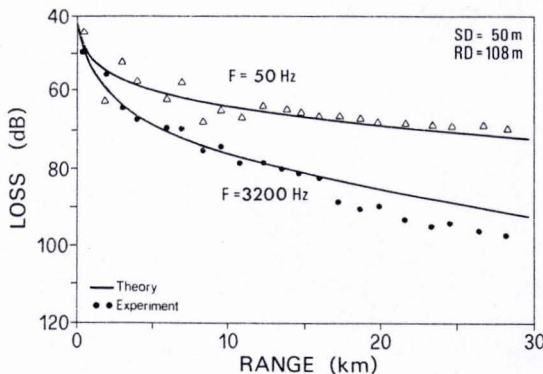


FIG. 9. Loss versus range at two different frequencies.

information retained. The incoherent loss computation corresponds to assigning a uniformly distributed random phase to each of the modes. An example of both coherent and incoherent loss versus range is given in Fig. A1. Here the rapidly oscillating curve displaying the multipath interference structure characteristic of ducted propagation is the coherent loss curve, while the smoothly decaying curve is the incoherent loss curve. We see that the smooth curve represents an accurate mean of the rapidly oscillating curve. This is an important result, since only the mean (incoherent) curve represents a stable answer to propagation in a given environment. Thus, any slight change in frequency, source/receiver geometry, or in the environmental inputs would cause a change in the multipath interference structure, which could lead to drastic changes in computed propagation loss at any given point in space. The mean level, on the other hand, would be relatively unaffected by perturbations in the various input parameters. Hence, when modeling propagation in shallow water, it is preferable to represent the acoustic field by incoherent addition of modes.

Figure A1 also displays experimentally measured propagation loss data (dots). In this case the data are averaged within a $\frac{1}{3}$ -octave band centered around 400 Hz. Excellent agreement is obtained between computed and measured losses, with the experimental data scattered around the smooth incoherent loss curve. We see that the data show less variation from the mean than indicated by the coherent loss curve. This is due to the fact that the data are band averaged, while the theoretical curve is a narrow-band result. To illustrate in more detail the effect of band averaging on the computed propagation loss, we are going to investigate the behavior of loss versus frequency within a $\frac{1}{3}$ -octave band centered around 400 Hz.

B. Third-octave band averaging

Figure A2 shows computed transmission loss versus frequency for both coherent and incoherent addition of modes at two different ranges, 2 and 20 km. Computations were done in steps of 1 Hz within the $\frac{1}{3}$ -octave band centered around 400 Hz. We see that the strongly fluctuating coherent loss curve has excursions from the mean of the same order of magnitude whether plotted versus range or frequency (Figs. A1 and A2). We

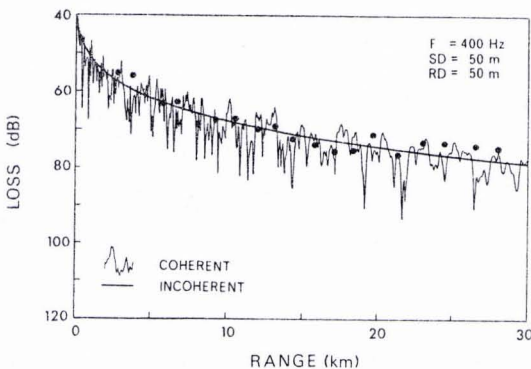


FIG. A1. Computed loss versus range by coherent and incoherent addition of modes. Dots are experimental data.

also see from Fig. A2 that the incoherent loss curve is smoothly varying with frequency, and that it represents a mean curve for the coherent loss. In fact, it can be shown numerically that a computed third-octave average loss by coherent and incoherent addition of modes gives almost identical results. However, while many points are necessary for an accurate sampling of the coherent loss curve, an average value can be obtained from the incoherent curve using very few sample points. Actually, in many cases the incoherently computed loss at the center frequency closely represents the third-octave band average. Only in the case of highly variable propagation conditions with frequency (channel resonance) is the above approach to band averaging inaccurate; this case is discussed in Sec. C.

A final remark on the data/model comparison in Fig. A1. We have shown that a band-averaged result is close to the incoherent result at the center frequency. Thus we should expect the data in Fig. A1 to show the same smooth behavior with range as the incoherent loss curve. This is not quite the case, for two reasons: first, the ocean is varying in both time and space, which naturally causes some fluctuations around the computed mean. Second, the source depth is not well defined, since the explosive charge detonates at slightly different depths from shot to shot. This also leads to fluctuations around the mean level with range. In any case, a meaningful comparison can generally be done between band-averaged experimental data and model outputs at the center frequency when using incoherent addition of modes.

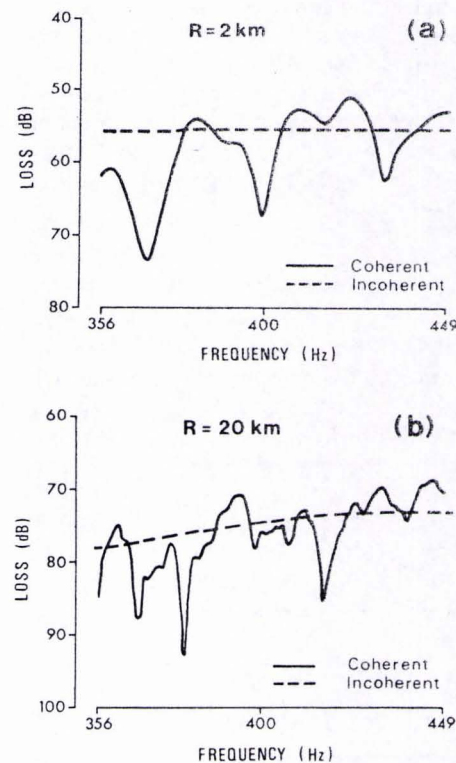


FIG. A2. Computed loss within a third-octave band at short and long ranges. Source and receiver at 50 m.

C. Channel resonance

Propagation loss predictions obtained by incoherent addition of modes will under particular environmental conditions exhibit strong level fluctuations with frequency. This so-called resonance phenomenon can become a quite serious problem in deterministic modeling since level fluctuations of 15 dB or more within a few hundred hertz are not uncommon. The problem arises whenever a secondary sound channel is present, which allows for propagation of a well-trapped mode at particular frequencies. The problem is illustrated schematically in Fig. A3. The main propagation channel is here the lower part of the water column, where the sound speed is lowest. The secondary channel is the isovelocity surface layer. Due to the speed difference between the two layers a critical angle exists for propagation from the lower to the upper channel. This means that shallow rays (1) originating from a source in the upper channel will propagate entirely in the lower channel, while steep rays (2) will propagate in both channels. Now, for a source or a receiver in the upper channel only rays of type (2) are important. For these rays the minimum loss occurs exactly when the ray angle at the interface between the lower and the upper channel is just beyond the critical angle. Steeper rays have higher loss (more bottom bounces between source and receiver), and shallower rays do not enter the upper channel at all. Thus the optimum propagation conditions occur when a ray (mode) with minimum loss exists. Due to the discreteness of ducted propagation, such a low-loss ray (mode) can exist only at specific frequencies. At intermediate frequencies the loss increases giving rise to highly variable propagation conditions with frequency.

As a simple example of channel resonance we have computed dispersion curves and propagation loss for the environment shown in Fig. A3. The environmental parameters used were the following: a 25-m surface layer with a speed of 1525 m/s and a 50-m main channel with a speed of 1500 m/s. The bottom speed was taken to be 1650 m/s, the density of 2 g/cm³, and the attenuation 1 dB/wavelength.

The dispersion curves for modes 4 to 13 are given in Fig. A4, exhibiting a sequence of group velocity maxima, one for each mode. At these maxima the group velocity approaches the speed of the upper channel (1525 m/s), which means that the mode is propagating almost entirely in that channel and therefore having only little interaction with the ocean bottom. Thus the group velocity maxima correspond to modes having

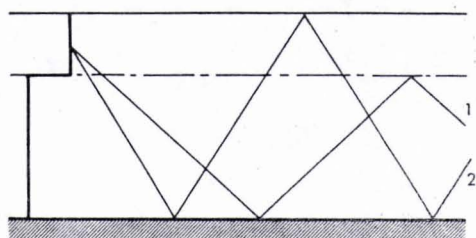


FIG. A3. Schematic of sound propagation in layered ocean.

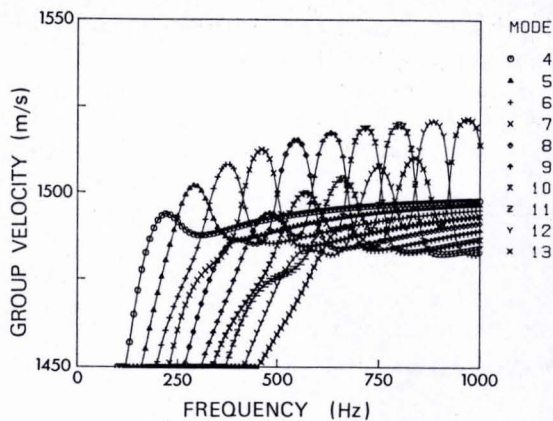


FIG. A4. Dispersion curves for modes 4 to 13.

minimum loss, which again means optimal propagation for either source or receiver in the upper channel. We see that the optimal propagation conditions in this case occur every 85 Hz.

The computed propagation loss by incoherent addition of modes is shown in Fig. A5 for various source/receiver combinations and for various ranges. For both source and receiver in the secondary channel [Fig. A5(a)] a strong resonance is evident at a range of 30 km with loss variations of around 15 dB. The resonance period is around 85 Hz, and good propagation coincides with the existence of a well-trapped mode in the upper channel as demonstrated on the dispersion curve plots (Fig. A4). We see that the resonance is much less pro-

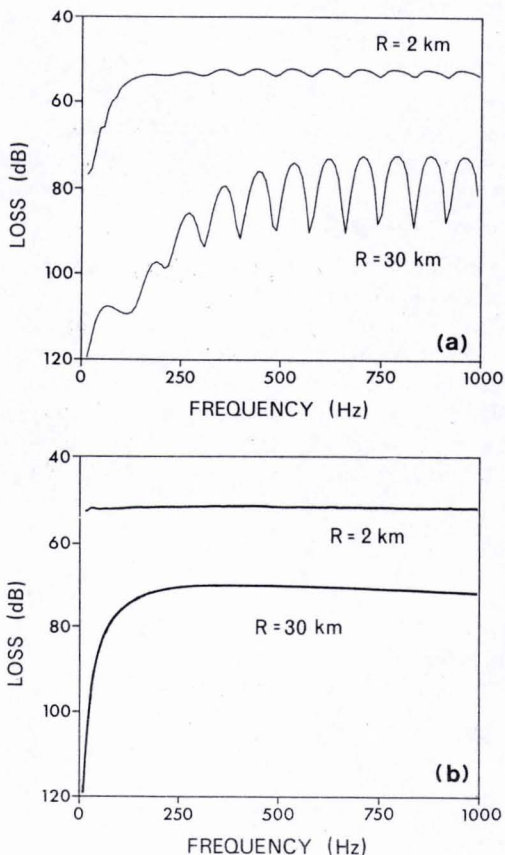


FIG. A5. Computed loss versus frequency for environment given in Fig. A3. (a) Source and receiver both at 10 m, and (b) source and receiver both at 50 m.

nounced at short ranges than at long ranges. Actually, the amplitude of variation of the resonance pattern increases with range, since the phenomenon is closely related to the presence of bottom loss. Hence resonance does not occur for propagation over an ideal nonlossy bottom. Figure A5(b) shows that no resonance is present when both source and receiver are in the main channel. Thus we may conclude that resonance only occurs when bottom loss is significant and either source or receiver is in a secondary propagation channel, and then only at long ranges.

Before proceeding to indicate solutions to the problem of resonance in acoustic modeling, we will show one more example using the model environment from the trial zone (Fig. 4 of main text). In this case, the main channel (lowest speed) is the sediment layer. Hence, with source and receiver in the water column, we should expect resonance to appear in the model prediction. The computed loss versus frequency by incoherent addition of modes is shown in Fig. A6 for a source depth of 50 m and for three different receiver depths. The resonance is clearly seen in the lower curve for a receiver 1 m above the bottom. While the data (dots) show a smooth behavior with frequency, the theoretical curve exhibits a typical resonance pattern with excursions of more than 10 dB from the mean. Thus we predict extremely poor propagation at 800 Hz and also around 2000 Hz.

As pointed out earlier, the resonance is caused by the presence of an idealized main propagation channel in the bottom. This can be seen explicitly by computing the bottom reflection loss versus frequency. An example is given in Fig. A7 for a grazing angle of 8° . We see that the correlation between propagation loss (Fig. A6) and bottom loss (Fig. A7) is striking at this particular angle. Clearly, we should consider propagation at all grazing angles, which is done in Fig. A8. Here we show contoured reflection loss versus angle

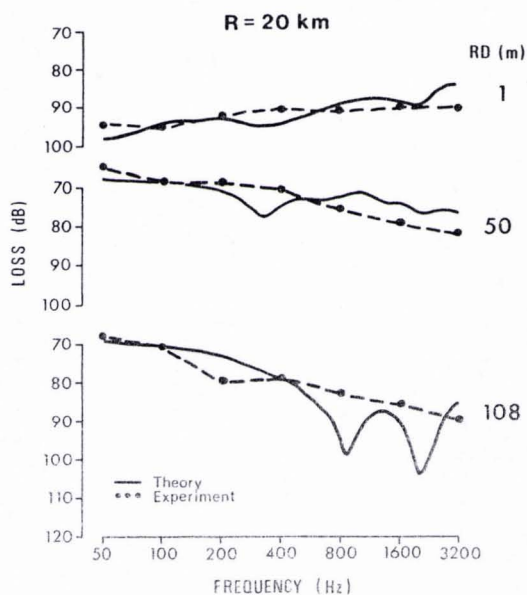


FIG. A6. Computed and measured loss versus frequency for different receiver depths.

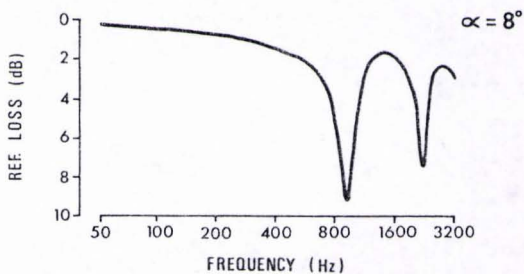


FIG. A7. Reflection loss versus frequency at a grazing angle of 8° .

and frequency as computed by a Thompson-Haskell bottom-loss model.¹⁶ High-loss regions (>5 -dB loss) are shaded, and they are seen to occur only at higher frequencies. Thus it seems quite clear that resonance in this case is caused by the bottom layering.

The effect of bottom layering on propagation is shown in more detail in Fig. A9, where propagation loss has been computed for three different layerings. The difference between the three bottoms is only that the depth of the thin sand layer in Fig. 4 has been put to 1.5, 2.5, and 3.5 m, respectively. The result (Fig. A9) clearly shows the effect on the resonance pattern of changing the bottom layering. Of course the average curve has a much smoother behavior with frequency than any of the individual loss curves. Furthermore, the average result is in quite good agreement with the data, indicating that strong resonances do not occur in the real ocean where, of course, the horizontal stratification is imperfect. All theoretical curves presented in the main text of this paper have been obtained as an average prediction based on the above three bottoms.

We have seen that channel resonance occurs in theory whenever source or receiver is in a secondary propagation channel. Thus resonance occurs for a low-speed bottom when either source or receiver is close to the bottom. It also occurs for a Mediterranean summer profile with source or receiver in the mixed layer (surface channel). The resonance phenomenon, on the other hand, is not pronounced for high-speed bottoms, for winter profiles, or for summer profiles with source and receiver below the thermocline.

As pointed out earlier, the resonance is possible

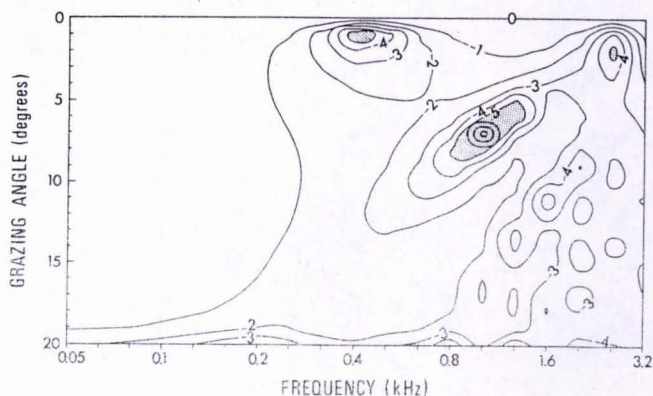


FIG. A8. Contoured reflection loss versus angle and frequency for bottom given in Fig. 4 of main text.

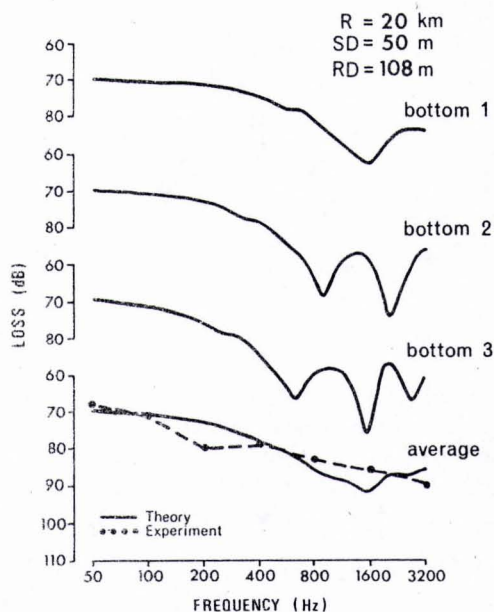


FIG. A9. Computed loss versus frequency for different bottom layerings.

only in a horizontally stratified geometry allowing for fixed well-defined propagation paths. In the real ocean, spatial and temporal variability break up the regularity sufficiently that these phenomena are seldom measured. One way of avoiding the resonance problem in deterministic modeling would be by using a range-dependent propagation model and vary the environmental inputs sufficiently along the propagation path. Another way of removing the resonance structure from the theoretical result would be by doing some kind of band averaging. If the resonance period is such that there are several oscillations within a third-octave band, a band average would give a smooth loss curve versus frequency. However, many frequency samples are required, which means long computer times. A third solution is the one used here, where losses have been averaged for a few environments created as perturbations on the nominal environment. This approach seems to be the most economical, since as few as three environments can be used in computing the average. However, the most physical solution is definitely the first one, namely the use of a range-dependent propagation model. This method also constitutes a practical solution to the modeling of broadband data, since, with resonance phenomena absent, a band-averaged result can be simulated by just doing a single-frequency, incoherent field calculation.

- ¹R. H. Ferris, "Comparison of Measured and Calculated Normal-Mode Amplitude Functions for Acoustic Waves in Shallow Water," *J. Acoust. Soc. Am.* 52, 981-988 (1972).
- ²F. Ingenito, "Measurements of Mode Attenuation Coefficients in Shallow Water," *J. Acoust. Soc. Am.* 53, 858-863 (1973).
- ³F. Ingenito and S. N. Wolf, "Acoustic Propagation in Shallow Water Overlying a Consolidated Bottom," *J. Acoust. Soc. Am.* 60, 611-617 (1976).
- ⁴F. Ingenito, R. H. Ferris, W. A. Kuperman, and S. N. Wolf, "Shallow Water Acoustics: Summary Report," NRL Rep. 8179, Nav. Res. Lab., Washington, DC (1978).
- ⁵C. T. Tindle, K. M. Guthrie, G. E. Bold, M. D. Johns, D. Jones, K. O. Dixon, and T. G. Birdsall, "Measurements of the Frequency Dependence of Normal Modes," *J. Acoust. Soc. Am.* 64, 1178-1185 (1978).
- ⁶E. L. Murphy, A. Wasiljeff, and F. B. Jensen, "Frequency-Dependent Influence of the Sea Bottom on the Near-Surface Sound Field in Shallow Water," *J. Acoust. Soc. Am.* 59, 839-845 (1976).
- ⁷L. A. Rubano, "Acoustic Propagation in Shallow Water over a Low-Velocity Bottom," *J. Acoust. Soc. Am.* 67, 1608-1613 (1980).
- ⁸M. C. Ferla, G. Dreini, F. B. Jensen, and W. A. Kuperman, "Broadband Model/Data Comparisons for Acoustic Propagation in Coastal Waters," in *Bottom-Interacting Ocean Acoustics*, edited by W. A. Kuperman and F. B. Jensen (Plenum, New York, 1980), pp. 577-592.
- ⁹J. H. Beebe and S. T. McDaniel, "Geoacoustic Models of the Seabed to Support Range-Dependent Propagation Studies on the Scotian Shelf," in *Bottom-Interacting Ocean Acoustics*, edited by W. A. Kuperman and F. B. Jensen (Plenum, New York, 1980), pp. 507-523.
- ¹⁰D. D. Ellis and D. M. F. Chapman, "Propagation Loss Modelling on the Scotian Shelf: Comparison of Model Predictions with Measurements," in *Bottom-Interacting Ocean Acoustics*, edited by W. A. Kuperman and F. B. Jensen (Plenum, New York, 1980), pp. 541-555.
- ¹¹F. B. Jensen and M. C. Ferla, "SNAP: the SACLANTCEN Normal-Mode Acoustic Propagation Model," Rep. SM-121, SACLANT ASW Research Centre, La Spezia, Italy (1979).
- ¹²T. Akal, O. F. Hastrup, and O. V. Olesen (personal communication).
- ¹³F. B. Jensen, "Comparison of Transmission Loss Data for Different Shallow-Water Areas with Theoretical Results Provided by a Three-Fluid Normal-Mode Propagation Model," in *Sound Propagation in Shallow Water*, edited by O. F. Hastrup and O. V. Olesen, Rep. CP-14 (SACLANT ASW Research Centre, La Spezia, Italy, 1974).
- ¹⁴F. B. Jensen and W. A. Kuperman, "Environmental Acoustic Modelling at SACLANTCEN," Rep. SR-34, SACLANT ASW Research Centre, La Spezia, Italy (1979).
- ¹⁵A. Skretting and C. C. Leroy, "Sound Attenuation between 200 Hz and 10 kHz," *J. Acoust. Soc. Am.* 49, 276-282 (1970).
- ¹⁶O. F. Hastrup, "Reflection of Plane Waves from a Solid Multilayered Damping Bottom," Rep. TR-50, SACLANT ASW Research Centre, La Spezia, Italy (1966).

INITIAL DISTRIBUTION

	Copies		Copies
<u>MINISTRIES OF DEFENCE</u>		<u>SCNR FOR SACLANTCEN</u>	
MOD Belgium	2	SCNR Belgium	1
DND Canada	10	SCNR Canada	1
CHOD Denmark	8	SCNR Denmark	1
MOD France	8	SCNR Germany	1
MOD Germany	15	SCNR Greece	1
MOD Greece	11	SCNR Italy	1
MOD Italy	10	SCNR Netherlands	1
MOD Netherlands	12	SCNR Norway	1
CHOD Norway	10	SCNR Portugal	1
MOD Portugal	5	SCNR Turkey	1
MOD Turkey	5	SCNR U.K.	1
MOD U.K.	16	SCNR U.S.	2
SECDEF U.S.	61	SECGEN Rep. SCNR	1
		NAMILCOM Rep. SCNR	1
<u>NATO AUTHORITIES</u>		<u>NATIONAL LIAISON OFFICERS</u>	
Defence Planning Committee	3	NLO Canada	1
NAMILCOM	2	NLO Denmark	1
SACLANT	10	NLO Germany	1
SACLANTREPEUR	1	NLO Italy	1
CINCWESTLANT/COMOCEANLANT	1	NLO U.K.	1
COMIBERLANT	1	NLO U.S.	1
CINCEASTLANT	1		
COMSUBACLANT	1	<u>NLR TO SACLANT</u>	
COMMAIREASTLANT	1	NLR Belgium	1
SACEUR	2	NLR Canada	1
CINCNORTH	1	NLR Denmark	1
CINCSOUTH	1	NLR Germany	1
COMNAVSOUTH	1	NLR Greece	1
COMSTRIKFORSOUTH	1	NLR Italy	1
COMEDCENT	1	NLR Netherlands	1
COMMARAIRED	1	NLR Norway	1
CINCHAN	1	NLR Portugal	1
		NLR Turkey	1
		NLR UK	1
		NLR US	1
		Total initial distribution	236
		SACLANTCEN Library	10
		Stock	<u>34</u>
		Total number of copies	280

